

ORIGINAL ARTICLE

Correlating Finite Element Model of a Car Spot-welded Front-End Module in the Light of Modal Testing Data

W.I.I. Wan Iskandar Mirza¹, M.N. Abdul Rani*¹, M.A. Yunus¹, B. Athikary² and M.S.M. Sani³

¹Structural Dynamics Analysis and Validation, Faculty of Mechanical Engineering, Universiti Teknologi MARA, Malaysia

²MSC Software Corporation India Pvt. Ltd, Pune Maharashtra, 411001 India

³Advanced Structural Integrity and Vibration Research (ASIVR), Faculty of Mechanical Engineering, Universiti Malaysia Pahang, 26600 Pekan, Pahang, Malaysia

ABSTRACT – Model updating methods can be adopted to improve the correlation level between the finite element model of a spot welded structure and its test model. However, in the presence of contact interfaces in the vicinity of the welded areas, improving the correlation level is problematic and challenging. An approach for correlating the finite element model of a welded structure with contact interfaces using finite element model updating and modal testing is proposed. The proposed approach was tested on a car front-end module structure that consisted of nine components and 76 resistance spot-welded joints used to assemble the components. CWELD and CELAS1 element connectors were used to represent the spot-welded joints and contact interfaces in the finite element modelling and updating. This approach was applied successfully to predict the modal parameters of the car spot-welded front-end module. The total error of the initial finite element model of the structure was reduced from 27.13% to 5.75%. The findings of this work suggest that the proposed approach has a great potential for use in investigating the dynamic behaviour of various spot-welded structures without a significant decline in accuracy.

ARTICLE HISTORY

Revised: 29th May 2020

Accepted: 29th June 2020

KEYWORDS

Finite Element Modelling,

Model updating,

Spot-welded joints,

Contact interface,

Spring element

INTRODUCTION

Developing accurate mathematical modelling of an assembled structure with welded joints for the prediction of dynamic behaviour is very challenging and has been extensively studied by many researchers [1-3]. Researchers attempt to such develop mathematical modelling using analytical methods, but these methods have been perceived as ineffective and expensive for large complex assembled structures which are prevalent in the automotive and aerospace industries [4, 5]. Several researchers have postulated that the use of the finite element method could be more effective than analytical methods since the finite element method can take complex boundary conditions into account as well as dealing with 2D and 3D domains [6]. In addition, several researchers [7-9], have shown that 1D element connectors can represent spot-welded joints in the structures.

The two 1D element connectors that have been widely used by researchers to represent spot-welded joints are ACM2 and CWELD. The former, which was proposed by [10] consists of a brick element which is connected to the upper and lower parts of the plate via RBE3. In contrast, the latter proposed by [11] is a special shear and flexible beam-type element with two nodes (CWELD) and twelve degrees of freedom. Other 1D element connectors derived from the finite element method are not an attractive option to be used for the modelling of spot-welded structures [12].

The use of ACM2 and CWELD element connectors for modelling and predicting the dynamic behaviour of welded structures has been demonstrated by [13]. However, its purpose was only carried out for a welded hat-plate in which the configurations were simple. Although it was performed on a relatively simple welded structure, the results obtained from the developed finite element models were found to be largely inconsistent with its experimental modal analysis (EMA) counterparts.

One way to improve the correlation between finite element models and test models is to use finite element model updating. This method is systematically used to reconcile finite element models with test models. The theoretical explanation of the model updating method is discussed in [14], and the use of the method in improving the finite element models in various applications are presented in [15, 16]. There has been extensive research related to model updating of assembled structures, particularly of welded joints. For instance, the model updating method was used to identify the material properties of friction stir welding in a dissimilar material plate structure [17]. Another striking example is the successful use of the model updating method to identify the complex parameters of laser spot-welded joints [18] by reconciling the diameters and the material properties of the welded regions with their experimental counterparts.

Previous studies [15-18] showed that model updating methods were effectively and successfully used to improve the joint parameters of the finite element models under study. However, modelling of welded joints requires a special approach [19, 20]. Little attention has been paid to modelling of the effects of contact interfaces. For instance, if the

welded structure has large contact interfaces, especially in the vicinity of the welded areas, the contact interfaces may highly affect the dynamic behaviour of the structure.

The contact interfaces of spot-welded joints in a welded structure seem to be large; this happens because welded joints are normally a surface to surface connection. Usually, researchers or engineers tend to completely ignore the contact interfaces during the modelling of the joints. This is because the properties of the contact are extremely difficult to determine accurately [21]. Therefore, the model updating method in the light of modal testing is seen to be a promising method to be employed in identifying the unknown parameters of the contact interfaces [22]. This paper presents an approach to correlating the finite element model of the welded structure with contact interfaces using finite element model updating and experimental modal analysis.

The proposed approach is performed on a car front end module structure that consists of nine components which are assembled by 76 resistance spot-welded joints. The front-end module, as shown in Figure 1 was used as a case study because its configuration is one of the primary sources of vibration in the car.



Figure 1. The front-end module of a car body in white.

Description of the Test Structure

The test module shown in Figure 2, consisted of nine components which were assembled using 76 resistance spot-welded joints. The components were made of galvanised steel, and the thicknesses were in the range between 1 mm and 1.4 mm. The length and total weight of the assembled front-end module were 960 mm and 2.45 kg, respectively.

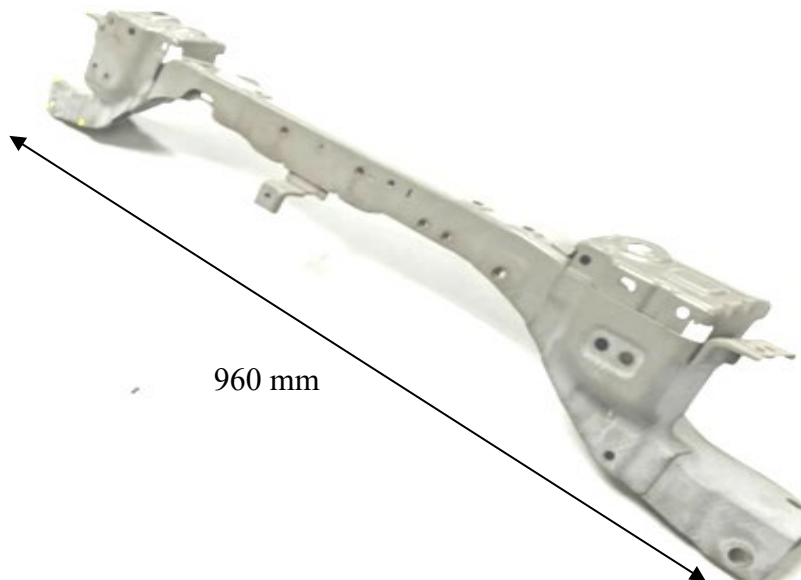


Figure 2. The test car front-end module.

The modal parameters (natural frequencies and mode shapes) predicted from the finite element model of the welded module were validated against the measured counterparts obtained from the experimental modal analysis (EMA) or modal testing for validation and model updating purposes. The test module was modelled and tested under free-free boundary conditions in accordance with previous studies [23, 24]. The frequency of interest used for the investigation was between 10 Hz and 500 Hz, of which several bending and torsional modes used in the model updating were measured. The rigid body modes were, however, neglected during the investigation.

FINITE ELEMENT MODELLING AND EXPERIMENTAL MODAL ANALYSIS OF THE TEST STRUCTURE

Figure 3 shows the FE model of the car front-end module. 2D shell elements were used for the development of the FE model. The size of the elements used in the FE model varied from 5 mm to 8 mm due to the complexity of the geometry of the test module. In total, the FE model of the test module consisted of 5530 elements and 6010 nodes. The standard material properties for the galvanised steel [25] was defined as follows; Young's modulus of 210,000 MPa, Poisson's ratio of 0.3, and density of 7.850 kg/m³. Normal modes analysis was performed on the finite element model.

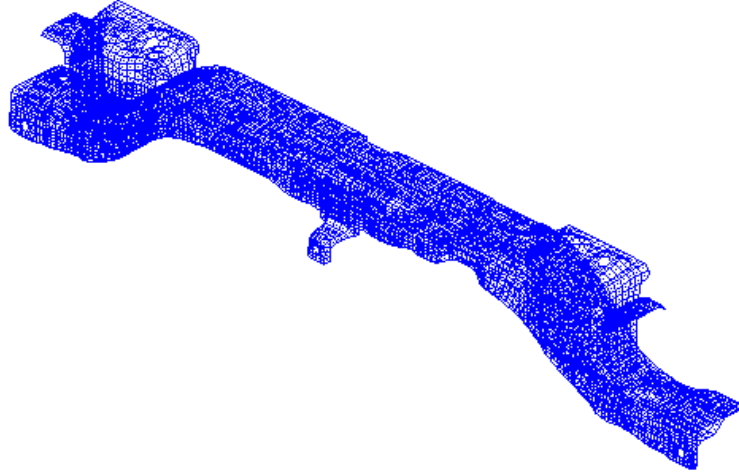


Figure 3: The finite element model of the car front-end module.

Modelling the Spot-welded Joints with CWELD Element Connectors

Previous studies [6, 21] revealed that one of the main challenges in finite element modelling was the modelling of joints. The main challenges encountered are attributed to the difficulty in determining the mechanical properties of the joints that are not only very complex but are case dependent [19]. Meanwhile, there are several types of element connectors that are available in commercial software packages, in which each of the element connectors has a different mathematical method representing the joints. Therefore, appropriate element connectors should be properly selected to accurately represent spot-welded joints in welded structures.

In recent years, structural dynamicists tend to use contact-area models that are (ACM2) and CWELD element connectors to represent spot-welded joints. The ACM2 element is a combination of several rigid body elements (RBE3) and brick elements. This enables spot welds to be located anywhere independently of the mesh areas. The use of RBE3 elements in ACM2 provides the advantage of the distribution of loads across surrounding shell nodes and the preservation of the value of the local stiffness. On the other hand, the CWELD element connector represents the welded joint by a single 1D element. The stiffness of the CWELD element connector is calculated from the material properties and the diameter of the element. The guidelines on how to model the ACM2 and CWELD element connectors in the finite element modelling are available in [9].

The CWELD element connector is seen to have an advantage over the ACM2 element connector because the diameter of the defined CWELD can be optimised and does not introduce any additional mass to the finite element model. In addition, it has been shown that the CWELD element connectors were found to be more capable of representing spot-welded joints compared with the ACM2 element connectors [26]. Therefore, the element connectors used in this work to represent spot-welded joints in the car front-end module are CWELD. Figure 4 shows the finite element model of the test module using CWELD element connectors. The material properties of the CWELD element are tabulated in Table 1. The natural frequencies and mode shapes of the finite element model of the test module are calculated using NASTRAN solution 103 (normal modes analysis). The range of frequency of the calculation is between 10Hz and 500Hz, and the rigid body modes are neglected.

Table 1. Material properties of CWELD.

Property	Value
Young's modulus	210,000 MPa
Poisson's ratio	0.3
Density	7850 kg/m ³
Diameter	5.00mm

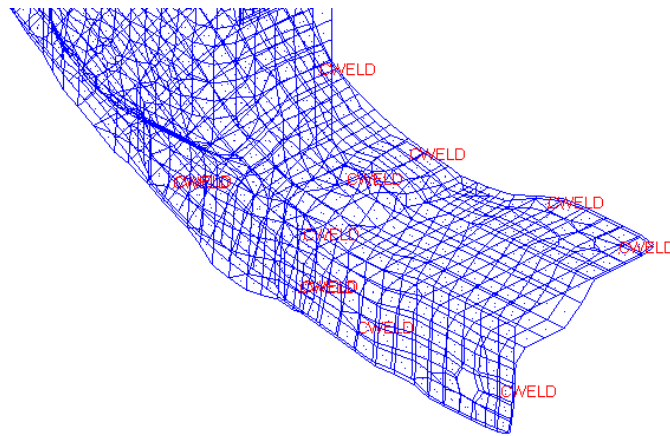


Figure 4. CWELD element connectors representing spot-welded joints in the test front-end module.

Experimental Modal Analysis

In this work, the natural frequencies and mode shapes of the test module were measured using experimental modal analysis (EMA). The experimental work was carried out by suspending the test module with two soft springs to simulate a free-free configuration. This experimental configuration was designed as to the finite element model. Figure 5 illustrates the experimental set-up of the test module in which a 21.65 mV/N impact hammer and three 10mV/g uniaxial accelerometers were used for the measurement. Dynamic data were acquired using the Measurement System (LMS) SCADAS. A frequency bandwidth was set between 0 Hz and 512 Hz with a frequency resolution of 0.5 Hz.

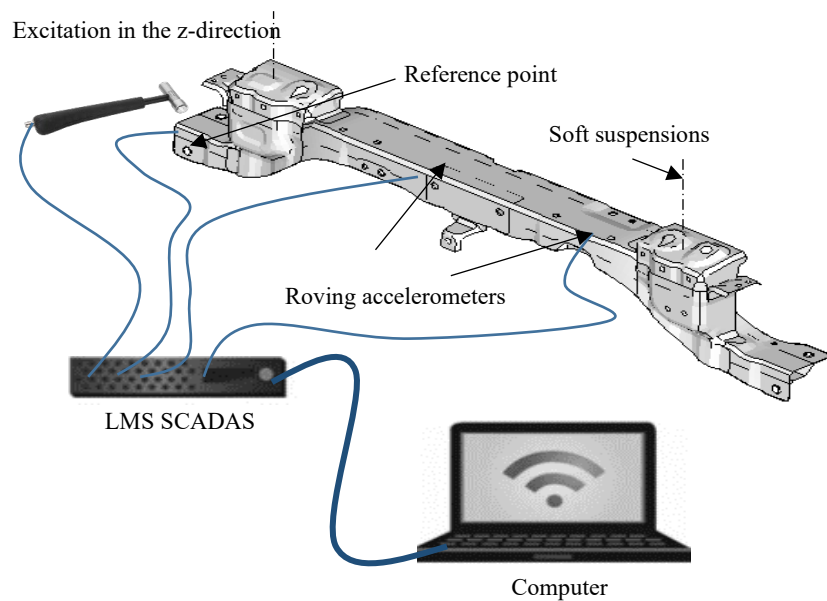


Figure 5. Experimental set-up of the test car front-end module.

Figure 5 shows the excitation reference point used to excite the car front-end module during the experimental modal analysis. Fifty-two measurement points were unidentified while two roving accelerometers measured the responses of the 52 points. To obtain reliable data, the structure was properly excited ten times, and their responses were then analysed using the LMS Testlab, while the frequency response functions (FRFs) were obtained by a least-mean squares curve-fitting procedure. Figure 6 presents the reference point’s FRF of the test car front-end module.

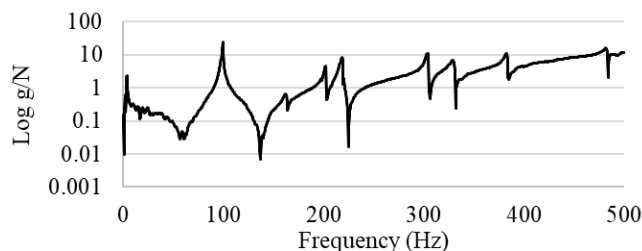


Figure 6. Reference point’s FRF of the test car front-end module.

The quality of the FRF measured from the excitation point FRF was analysed by observing the results of the coherence function. Quality is acceptable if the coherence value approaches 1.0. Figure 7 presents the coherence function obtained from the reference point. Averaging the results of 10 multiple excitations as in Figure 7 shows a good coherence value close to 1.0.

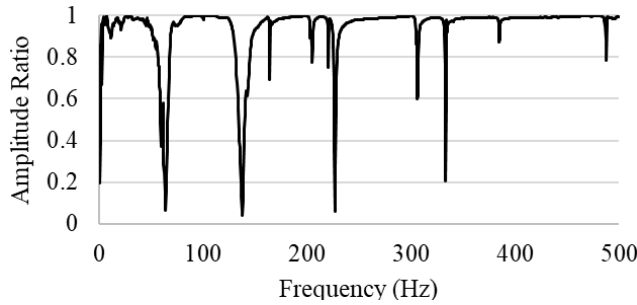


Figure 7. Reference point's coherence of test car front-end module

Figure 8 shows the sum of FRFs of 52 measurement points presented from eight modes identified within the frequency range of interest. The measured natural frequencies and mode shapes of the test car front-end module are presented and discussed in the next section.

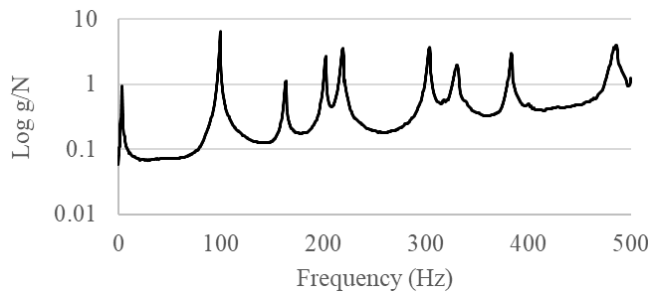


Figure 8. The sum FRF of the test car front-end module

MODEL VALIDATION AND UPDATING OF THE INITIAL FINITE ELEMENT MODEL OF THE TEST MODULE

Accuracy of the developed finite element model was evaluated by comparing the calculated modal parameters with their measured counterparts. Modal assurance criterion (MAC) was performed in order to quantify the accuracy of the mode shapes since the geometry of the structure can be considered as complex. Information on the MAC analysis can be found in [27]. The governing equation for MAC is as follows:

$$MAC(\varphi_{test}, \varphi_{FE}) = \frac{|\langle \varphi_{test}, \varphi_{FE} \rangle|^2}{(\langle \varphi_{test}, \varphi_{test} \rangle)(\langle \varphi_{FE}, \varphi_{FE} \rangle)} \tag{1}$$

where φ_{test} and φ_{FE} are test and finite element modal vectors respectively. Generally, the diagonal values of MAC that are close to 100% express the similarity between the finite element and measured mode shapes. In this work, eight modes were determined from the finite element model and EMA. A comparison of the modal parameters (natural frequencies and mode shapes) in terms of percentage error and MAC value between the initial finite element model and EMA is tabulated in Table 2.

Table 2. Comparison of natural frequencies between Initial FE model and EMA.

Mode	Initial FE (Hz)	EMA (Hz)	Error. (%)	MAC (%)
1	100.29	98.78	1.53	97.80
2	164.22	162.12	1.30	91.90
3	200.80	201.37	0.28	90.50
4	223.25	217.89	2.46	89.00
5	305.37	302.15	1.07	92.90
6	344.18	328.94	4.63	89.20
7	442.56	382.65	15.66	2.60
8	484.42	483.46	0.20	28.10
Total error (%)			27.13	

A lack of correlation was recorded between the natural frequencies of initial FE and EMA, especially for the 4th, 6th and 7th modes. In contrast, a high MAC value in mode shapes was calculated except for the 7th and 8th mode. The 7th mode

with 15.66 % of error is the biggest contributor to the total error of 27.13 %. The mode also recorded the lowest MAC value of 2.60 %. However, a surprising finding was found in the 8th mode in which a different achievement level was recorded in the FE natural frequency and mode shape. The FE natural frequency showed very good agreement with its EMA counterpart (0.20 %), whereas the FE mode shape registered a poor MAC value of 28.10 %.

The degree of similarity of mode shapes between the initial FE model and EMA was analysed using the MAC analysis, and the diagonal MAC values for the mode shapes are presented in Table 3. It is clearly shown that very low MAC values were found in the 7th and 8th modes with 2.6 and 28.1 % respectively. On the other hand, the 7th mode of the initial FE model bore some similarity to the 8th mode of EMA. This indicated that there was a mode pairing problem between the FE with EMA, in particular for the 7th and 8th modes. The reason behind this scenario may be due to erroneous assumptions about the material properties of the FE [12,21]. Therefore, model updating is required to improve the initial FE model of the front-end module.

Table 3. Comparison of MAC values between Initial FE (column) and EMA (row) mode shapes.

Mode	1	2	3	4	5	6	7	8
1	97.8	0.0	0.3	0.5	0.0	0.0	15.1	0.6
2	0.1	91.9	0.6	1.1	12.4	7.5	0.7	0.0
3	0.1	0.9	90.5	12.2	4.0	0.8	6.2	0.0
4	0.2	0.8	0.1	89.0	0.0	5.3	6.9	6.8
5	0.1	12.3	2.4	0.8	92.9	1.0	13.0	0.9
6	0.0	3.2	1.9	5.4	0.1	89.2	55.4	13.7
7	6.0	0.1	4.6	1.6	0.1	7.1	2.6	59.0
8	0.5	0.4	2.0	1.0	12.8	9.3	2.8	28.1

FINITE ELEMENT MODEL UPDATING METHOD

There have been attempts made to correlate finite element models with the experimental model by using the model updating method [8,15,18,19]. In general, the most common conclusion drawn is that sensitivity analysis is a very effective method of selecting potential updating parameters. The detailed explanation and tutorial of the sensitivity analysis can be found in [28]. The parameterisation can be performed using the sensitivity analysis in the form of;

$$S = \Phi_i^T \left[\frac{\delta K}{\delta \theta_j} - \omega_i \frac{\delta M}{\delta \theta_j} \right] \Phi_i \tag{2}$$

Where matrix S denotes the sensitivity matrix, while Φ , ω and θ denote the eigenvector, eigenvalue and parameter respectively, i indicates the i -th eigenvalue and j is the j -th parameter. The model updating method is performed by iteratively reconciling the parameters that are sensitive to the natural frequencies and MAC values. The iteration is completed as the discrepancies between the measured and predicted responses which are modal data, are minimised [14].

In this work, the material and geometrical properties of the components and the CWELD element connectors of the FE model were selected as updating parameters. The updating calculation was performed by using MSC NASTRAN Solution 200 with the same objective function used in [15,18]. Perturbations in the updating parameters were only allowed for plus-minus 10 % of the initial values defined. A comparison of the natural frequencies and the MAC values between the updated FE model and EMA is shown in Table 4.

Table 4. Comparison of natural frequencies between Updated FE model and EMA.

Mode	Updated FE (Hz)	EMA (Hz)	Error. (%)	MAC (%)
1	98.86	98.78	0.08	97.70
2	162.90	162.12	0.48	91.80
3	200.36	201.37	0.50	90.30
4	218.82	217.89	0.43	93.80
5	303.60	302.15	0.48	92.30
6	332.60	328.94	1.11	92.20
7	387.75	382.65	1.33	62.00
8	467.76	483.46	3.25	69.20
Total error (%)			7.66	

One of the main aims of this work was to improve the quality of the predicted results of the FE model of the front-end module. The achievement was evaluated by the degree of a reduction in the discrepancies between the FE and EMA. A significant reduction in the total error was recorded in the updated FE model. In other words, the total error of 27.13 % calculated from the initial FE model (Table 2) was reduced to 7.66 % as a result of a remarkable improvement of 91 % in the 7th mode (Table 4).

Another important achievement recorded was that the MAC values of the 7th and 8th modes were dramatically improved. However, a slight increment in the calculation of percentage error was found in the 8th mode, which is from

0.2 % to 3.25 %. The increment clearly showed that the updated FE model was incapable of accurately determining the 8th natural frequency. It is fair to conclude that the use of the updating parameters is quite insufficient in the attempt to improve the predicted natural frequencies.

The use of modal updating had reduced the value of Young's modulus of CWELD element to 199256 MPa. The reduction of Young's modulus was 5.11 % from the initial value of 210 000 MPa (refer Table 1). The updated value for the diameter of CWELD element was also reduced to 4.20 mm, which is 1.60 % reduction from the initial value of 5 mm.

INTRODUCING CONTACT SURFACE JOINTS AS UPDATING PARAMETER

As presented earlier, the updated natural frequency of the 8th mode recorded a slight increment in percentage error calculation. Therefore, an additional updating parameter; the spring elements were used to represent contact interfaces surrounding the spot-welded joints between the components of the test front-end module.

Finite Element Modelling of Contact Surface using CELAS1 Spring Element

CELAS1 is a scalar spring connection consisting of a single axial stiffness value. In the finite element modelling of contact interfaces, CELAS1 spring elements were used to connect both ends of CELAS1 to the contacting spot-welded surface points of the car front-end module. The stiffness of the spring was defined in the axial direction of CELAS1 elements. In practice, the properties of the contact interfaces are extremely difficult to be determined. Therefore, a small value of 100N/m of stiffness was initially used in the modelling. Also used in the modelling were the updated material and geometrical properties obtained from previous updating work. The use of CELAS1 elements in modelling the contact interfaces of the spot-welded joints is shown in Figure 9.



Figure 9. Contact Interfaces of car front-end module

The natural frequencies and mode shapes of the initial FE model with CELAS1 elements for the new finite element model were calculated by using the same normal modes solution. The natural frequencies and MAC values of the FE model were compared with its measured counterparts. Table 5 tabulates a comparison of these results. Table 6 presents the results of the MAC analysis.

A large discrepancy between the initial FE model with CELAS1 and EMA can be seen in the total error, which is 87.73 % in Table 5. In addition, the MAC values presented in Table 6 clearly shows a marked deterioration. It was found that the deterioration had directly led to a mode swapping problem in the 2nd, 3rd, 4th, 5th and 6th modes. Correlating an FE model mode with swapping problems can be extremely challenging.

It is worth concluding that the natural frequencies and mode shapes of the FE model with CELAS1 are sensitive to the spring elements used to represent the contact interfaces. Since the values of the stiffness of the spring elements were defined based on initial assumptions, model updating was carried out in the light of the test results to calculate the reasonable value of the stiffness systematically.

Table 5. Comparison of natural frequencies between initial FE model with CELAS1 and EMA.

Mode	FE with contact (Hz)	EMA (Hz)	Error. (%)	MAC (%)
1	95.917	98.78	2.90	35.80
2	106.93	162.12	34.04	0.00
3	184.29	201.37	8.48	3.70
4	220.81	217.89	1.34	8.10
5	232.77	302.15	22.96	0.40
6	324.13	328.94	1.46	4.60
7	359.12	382.65	6.15	67.60
8	433.19	483.46	10.40	32.50
Total error (%)			87.73	

Table 6. Comparison of MAC values (%) between the initial FE Model with CELAS1 (column) and EMA (row) mode shapes.

Mode	1	2	3	4	5	6	7	8
1	35.8	0.0	1.2	0.2	0.0	0.2	1.1	0.0
2	41.8	0.0	0.9	0.2	0.1	1.0	10.6	1.2
3	0.1	89.4	3.7	4.5	9.4	6.1	0.8	0.0
4	1.0	7.4	82.9	8.1	7.4	0.1	7.6	0.1
5	0.1	0.2	0.3	92.7	0.4	7.7	6.2	4.9
6	0.1	15.9	0.7	0.3	90.2	4.6	7.5	2.1
7	0.2	2.5	3.6	5.9	2.9	82.3	67.6	6.1
8	15.6	0.9	10.7	1.5	1.4	2.8	16.8	32.5

Updating the Surface Contact Joints

Model updating was performed on the FE model with CELAS1 by using the values of the stiffness of the spring elements as the updating parameter. The same objective function was used in updating. Each of the CELAS1 elements was updated individually. Through the use of the modal updating method, the stiffness value of CELAS1 elements decreased between 88.00 and 95.00 % of the initial value of 100 N/m. Table 7 presents a comparison of the modal parameters between the updated FE model with CELAS1 and EMA.

From Table 7, it can be clearly seen that the percentage error for individual modes was dramatically reduced, leading to a huge reduction in the total error of between 87.73 % and 5.75 %. The achievement was significant as it proved that the proposed model updating approach using spring elements as the updating parameter substantially improved the accuracy of the FE model. The advancement directly resulted in a significant improvement in the MAC values with an average MAC value of 88 % compared to the 19 % calculated from the initial FE model with CELAS1. Another intriguing advancement from the updating was that the MAC values of the 7th and 8th modes had significantly improved, thus ensuring that the mode swapping problem was successfully solved. Table 8 presents a comparison of percentage errors and MAC values between the updated FE model with and without CELAS1.

Table 7. Comparison of natural frequencies between Updated FE Model with CELAS1 and EMA.

Mode	Updated FE and contact (Hz)	EMA (Hz)	Error. (%)	MAC (%)
1	98.36	98.78	0.42	95.10
2	163.15	162.12	0.63	92.30
3	202.21	201.37	0.41	91.60
4	218.70	217.89	0.37	94.70
5	303.01	302.15	0.29	92.30
6	331.50	328.94	0.78	91.70
7	386.10	382.65	0.90	70.50
8	474.04	483.46	1.95	75.70
Total error			5.75	

Table 8. Comparison of MAC values (%) between Updated FE Model with CELAS1 (column) and EMA (row) mode shapes.

Mode	1	2	3	4	5	6	7	8
1	95.1	0.0	0.0	0.6	0.0	0.2	14.9	0.8
2	0.1	92.3	0.5	1.0	13.8	7.7	0.5	0.0
3	0.4	1.5	91.6	5.9	5.2	1.4	9.4	0.1
4	0.0	1.7	1.6	94.7	0.0	6.2	5.0	4.5
5	0.0	11.6	1.4	1.0	92.3	1.4	10.9	1.2
6	0.0	5.5	1.7	7.0	0.1	91.7	50.0	9.9
7	15.2	0.3	15.4	3.2	14.0	9.9	70.5	8.6
8	0.0	0.6	0.0	0.5	0.6	35.9	16.1	75.7

Table 9. Comparison of percentage errors and MAC values between the updated FE model with and without CELAS1.

Mode	Updated FE error. (%)	MAC (%)	Updated FE and contact error. (%)	MAC (%)
1	0.08	97.70	0.42	95.10
2	0.48	91.80	0.63	92.30
3	0.50	90.30	0.41	91.60
4	0.43	93.80	0.37	94.70
5	0.48	92.30	0.29	92.30
6	1.11	92.20	0.78	91.70
7	1.33	62.00	0.90	70.50
8	3.25	69.20	1.95	75.70
Total error (%)	7.66		5.75	

Table 10. Comparison of mode shapes between updated FE model with CELAS1 and EMA.

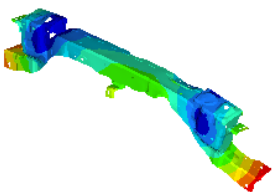
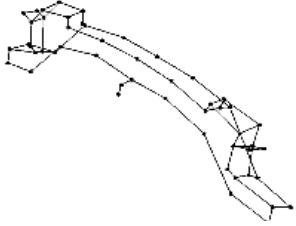
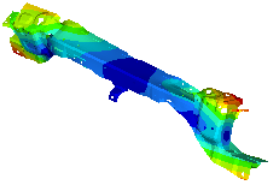
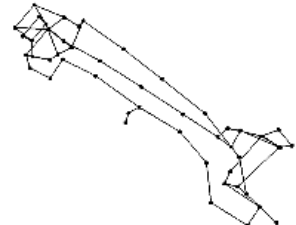
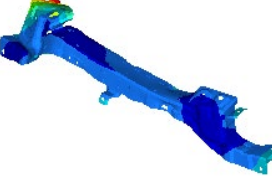
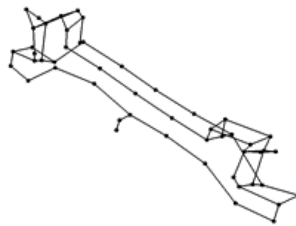
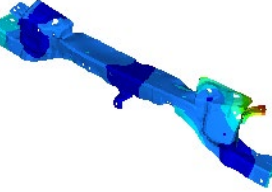
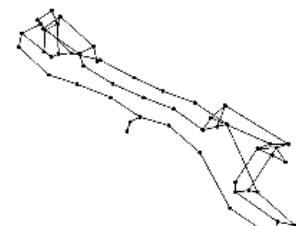
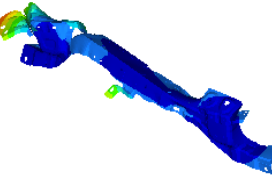
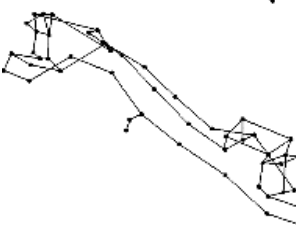
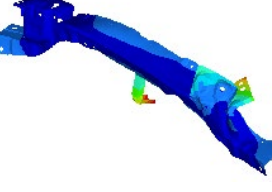
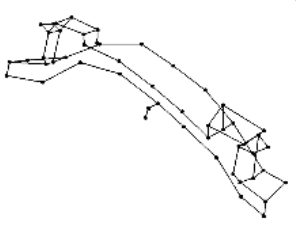
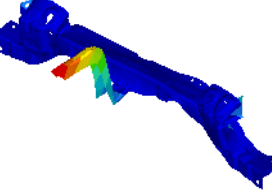
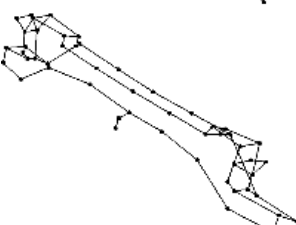
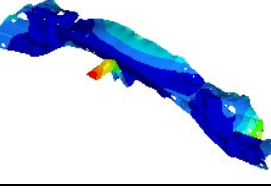
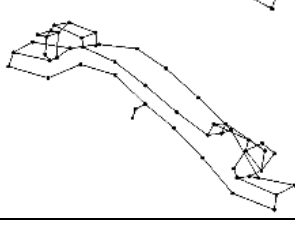
Mode	Updated FE	EMA
1		
2		
3		
4		
5		
6		
7		
8		

Table 9 clearly shows that the 8th FE natural frequency, the largest contributor to total error had significantly been reduced from 3.25 % to 1.95 %. This achievement revealed that modelling and updating the contact interfaces of the spot-welded joints helped to increase the reliability of the FE model in predicting the modal parameters of the test car front-end module. On top of that, the MAC values of the 7th and 8th modes increased by 13 % and 9 % respectively. A direct comparison of mode shapes between the updated FE model with CELAS1 and the measured counterparts is shown in Table 10. All modes were paired in the correct sequence without having missed modes or mode swapping problems. The comparison, therefore, clearly indicated that the updated FE model with CELAS1 was highly capable of accurately predicting the mode shapes of the car front-end module.

CONCLUSION

This paper presents a new approach to correlating the FE model of the car front-end module using model updating with contact interfaces as updating parameters and modal testing data. The use of model updating with CELAS1 and modal testing data was found to have tremendously improved the accuracy of the FE model in predicting the modal parameters of the car front-end module. The finding suggests that the effect of contact interfaces in the vicinity of the spot-welded joints should be included in modelling and also updating procedures. The proposed approach could be applied quite reliably to other complex structures with spot-welded joints without a significant decline in accuracy.

ACKNOWLEDGEMENT

The authors are gratefully indebted to the Malaysian Ministry of Higher Education for providing financial support for this study through the GIP grant scheme (600-IRMI 5/3/GIP (012/2019)). They would also like to express their gratitude for the help and support given by Prof. Ir. Dr Hj. Abdul Rahman Omar, Prof. Dr Hadariah Bahron, and SDAV group members.

REFERENCES

- [1] Souza JPB, Aguiar RAA, Costa HRM, Reis JML, Pacheco PMCL. Numerical modelling of the mechanical behavior of hybrid joint obtained by spot welding and bonding. *Composite Structures* 2018;202:216-21.
- [2] Krejsa M, Brozovsky J, Mikolasek D, Parenica P, Flodr J, Materna A, et al. Numerical modeling of steel fillet welded joint. *Advances in Engineering Software* 2018;117:59-69.
- [3] Wu G, Li D, Su X, Peng Y, Shi Y, Huang L, et al. Experiment and modeling on fatigue of the DP780GI spot-welded joint. *International Journal of Fatigue* 2017;103:73-85.
- [4] Noh W, Koh Y, Chung K, Song J-H, Lee M-G. Influence of dynamic loading on failure behavior of spot-welded automotive steel sheets. *International Journal of Mechanical Sciences* 2018;144:407-26.
- [5] Zhang CQ, Robson JD, Prangnell PB. Dissimilar ultrasonic spot welding of aerospace aluminum alloy AA2139 to titanium alloy TiAl6V4. *Journal of Materials Processing Technology* 2016;231:382-8.
- [6] Omar R, Rani MNA, Yunus MA, Starbuck DP, Mirza WIIWI, Zin MSM, editors. Different flexibility formulae for finite element modelling and analysis of the dynamic behaviour of a structure with bolted joints. *AIP Conference Proceedings* 2019 2059: 020004.
- [7] De Alba Alvarez RO, Ferguson NS, Mace BR. A robust spot weld model for structural vibration analysis. *Finite Elements in Analysis and Design*. 2014;89:1-7.
- [8] Yunus MA, Ouyang H, Abdul Rani MN, Mat Isa AA. Finite element modelling and updating of bolted joints in a thin sheet metal structure. In: 20th International Congress on Sound and Vibration 2013; 2: 1146-1152
- [9] Palmonella M, Friswell MI, Mottershead JE, Lees AW. Guidelines for the implementation of the CWELD and ACM2 spot weld models in structural dynamics. *Finite Elements in Analysis and Design* 2004;41(2):193-210
- [10] Heiserer D, Chargin M, Siela J, editors. High performance, process oriented, weld spot approach. In: 1st MSC Worldwide Automotive User Conference; 1999.
- [11] Fang J, Hoff C, B. Holman, Muller F, Wallerstein D, editors. Weld Modelling in MSC.Nastran. In: 2nd MSC Worldwide Automotive User Conference; 2000.
- [12] Sani MSM, Nazri NA, Rani MNA, Yunus MA, editors. Dynamic analysis of a cross beam section dissimilar plate joined by TIG welding. *AIP Conference Proceedings* 2018; 1952: 020086.
- [13] Husain NA, Khodaparast HH, Snaylam A, James S, Dearden G, Ouyang H. Finite-element modelling and updating of laser spot weld joints in a top-hat structure for dynamic analysis. *Proceedings of the Institution of Mechanical Engineers, Part C: Journal of Mechanical Engineering Science* 2010;224(4):851-61.
- [14] Mottershead JE, Friswell MI. Model updating in structural dynamics: A survey. *Journal of Sound and Vibration* 1993;167(2):347-75.
- [15] Simoen E, De Roeck G, Lombaert G. Dealing with uncertainty in model updating for damage assessment: A review. *Mechanical Systems and Signal Processing* 2015;56-57:123-49.
- [16] Panwar V, Gupta P, Bagha AK, Chauhan N. A review on studies of finite element model updating and updating of composite materials. *Materials Today: Proceedings* 2018;5(14, Part 2):27912-8.
- [17] Omar R, Abdul Rani MN, Yunus MA, Wan Iskandar Mirza WII, Mohd Zin MS. Efficient finite element modelling for the investigation of the dynamic behaviour of a structure with bolted joints. *AIP Conference Proceedings* 2019;1952: 020082.
- [18] Zin MSM, Rani MNA, Yunus MA, Sani MSM, Wan Iskandar Mirza WII, Mat Isa AA, editors. Frequency response function (FRF) based updating of a laser spot-welded structure. *AIP Conference Proceedings* 2018;1952: 020055.
- [19] Omar R, Rani MNA, Yunus MA, Isa AAM, Mirza WIIWI, Zin MSM, et al. Investigation of Mesh Size effect on dynamic behaviour of an assembled structure with bolted joints using finite element method. *International Journal of Automotive and Mechanical Engineering* 2018;15(3):5695-709.

- [20] Yunus MA, Abdul Rani MN, Sani MSM, Aziz Shah MAS. Finite element model updating of riveted joints of simplified model aircraft structure. AIP Conference Proceedings 2018; 1952: 020013.
- [21] Ahmadian H, Mottershead JE, James S, Friswell MI, Reece CA. Modelling and updating of large surface-to-surface joints in the AWE-MACE structure. Mechanical Systems and Signal Processing 2006;20(4):868-80.
- [22] Gant F, Rouch P, Champaney L. Updating of uncertain joint models using the Lack-Of-Knowledge theory. Computers and Structures 2013;128:128-35.
- [23] Abdullah NAZ, Sani MSM, Husain NA, Rahman MM, Zaman I. Dynamics properties of a Go-kart chassis structure and its prediction improvement using model updating approach. International Journal of Automotive and Mechanical Engineering 2017;14(1):3887-97
- [24] Mirza WIIWI, Rani MNA, Yunus MA, Ayub MA, Sani MSM, Mohd Zin MS. Frequency based substructuring for structure with double bolted joints: A case study. International Journal of Automotive and Mechanical Engineering 2019;16(1):6188-99.
- [25] Peter C, Abdul Rani MN, Starbuck DP, Yunus MA, Rezali KAM, Mohd Zin MS. Finite element modelling and analysis for dynamic investigation of a laser spot-welded hat-plate structure. IOP Conference Series: Materials Science and Engineering 2018;506(1):012065.
- [26] Zin MSM, Rani MNA, Yunus MA, Ayub MA, Sani MSM, Shah MASA, editors. Modal based updating for the dynamic behaviour of a car trunk lid. AIP Conference Proceedings 2019; 2059: 020001.
- [27] Pastor M, Binda M, Harčarik T. Modal Assurance Criterion. Procedia Engineering 2012;48:543-8.
- [28] Mottershead JE, Link M, Friswell MI. The sensitivity method in finite element model updating: A tutorial. Mechanical Systems and Signal Processing 2011;25(7):2275-96.